Т. 87, № 1 ЖУРНАЛ ПРИКЛАДНОЙ СПЕКТРОСКОПИИ ЯНВАРЬ — ФЕВРАЛЬ 2020
V. 87, N 1 JOURNAL OF APPLIED SPECTROSCOPY JANUARY — FEBRUARY 2020

SYNTHESIS OF NANO-URCHIN Mo-DOPED VO_2 PARTICLES BY THE HYDROTHERMAL METHOD

**N. T. Manh [1,2], N. T. Thanh [1,3], P. D. Tam [1,4*],
V. T. N. Minh [5], C. X. Thang [1], V.-H. Pham [1*]**

[1] Advanced Institute for Science and Technology (AIST), Hanoi University of Science and Technology (HUST), Hanoi, Vietnam; e-mail: vuong.phamhung@hust.edu.vn
[2] School of Engineering Physics, Hanoi University of Science and Technology (HUST), Hanoi, Vietnam
[3] Quy Nhon University, Quy Nhon, Binh Dinh, Vietnam
[4] Faculty of Material Science and Engineering, Phenikaa University, Yen Nghia, Hanoi 1000, Vietnam
[5] School of Chemical Engineering, Hanoi University of Science and Technology (HUST), Hanoi, Vietnam

This paper reports for the first time the synthesis of nano-urchin Mo-doped VO_2 particles and its degradation properties in the presence of methylene blue (MB). Nano-urchin Mo-doped VO_2 particles were synthesized by the hydrothermal method, and their microstructure was controlled by the concentration of Mo. The Mo-doped VO_2 particles showed fast degradation of methylene blue in a relatively short time of 5–10 min. These results show the potential application of Mo-doped VO_2 particles for decolorization of dyers in environmental water treatment.

Keywords: *VO_2, nanoparticle, hydrothermal, 3D structure, synthesis.*

СИНТЕЗ ГИДРОТЕРМАЛЬНЫМ МЕТОДОМ ЛЕГИРОВАННЫХ МОЛИБДЕНОМ НАНОЧАСТИЦ VO_2

**N. T. Manh [1,2], N. T. Thanh [1,3], P. D. Tam [1,4*],
V. T. N. Minh [5], C. X. Thang [1], V.-H. Pham [1*]**

УДК 535.42/.44:620.3

[1] Ханойский университет науки и технологии, Ханой, Вьетнам; e-mail: vuong.phamhung@hust.edu.vn
[2] Школа инженерной физики, Ханойский университет науки и технологии, Ханой, Вьетнам
[3] Куиненский университет, Куинен, Биндинь, Вьетнам
[4] Phenikaa Университет, Ханой, Вьетнам
[5] Школа химической инженерии, Ханойский университет науки и технологии, Ханой, Вьетнам

(Поступила 5 ноября 2018)

Гидротермальным методом синтезированы наночастицы VO_2, легированные молибденом, и исследована их способность вызывать разложение красителя метиленового голубого. Микроструктуру наночастиц контролировали по концентрации молибдена. Обнаружено, что легированные молибденом частицы VO_2 способны вызывать быстрое разложение метиленового голубого за относительно короткое время 5–10 мин. Результаты позволяют предположить, что частицы VO_2, легированные молибденом, можно применять для обесцвечивания красителей при очистке сточных вод.

Ключевые слова: *VO_2, наночастица, гидротермальный метод, 3D-структура, синтез.*

Introduction. Vanadium dioxide (VO_2) nanoparticle has attracted increasing attention because of its wide application in many fields, such as smart window coatings, lithium batteries, catalysts, gas sensors, and lasers [1, 2]. Various methods have used to synthesize VO_2 nanoparticles, such as thermal reduction [3], sol-gel [4, 5], microemulsion [6, 7], microwave [8], and hydrothermal methods [9, 10]. Among these methods, the hydrothermal method is of particular interest due to its simpliaty and cost-effectiveness [11, 12]. It has been reported that V_4O_9 nanoparticles [13] and V_2O_5 films [14] can be used in dye degradation for environmental water treatment. In particular, to our knowledge, there are no reports on the decolorization of methylene blue (MB) by nano-urchin Mo-doped VO_2 particles. Herein, a novel, nano-urchin Mo-doped VO_2 particle was synthesized successfully by the hydrothermal method. Nano-urchin VO_2 particles were controlled by modulating the Mo concentration. The nano-urchin Mo-doped VO_2 particle can induce fast degradation of MB in a very short time, 5–10 min. The phase and microstructure of the Mo-doped VO_2 particles were characterized by XRD diffraction and scanning electron microscopy (SEM). The decolorization of blue MB by Mo-doped VO_2 particles was determined by UV-Vis spectrometer.

Experimental procedure. Molybdenum (Mo)-doped VO_2 particles were synthesized through a hydrothermal method, as follows: an aqueous solution containing x mol of ammonium molybdate tetrahydrate $(NH_4)_6Mo_7O_{24}.4H_2O$ (99.99% purity, Merck), $x = 0, 5, 8, 10, 14$, and 20, was added to an aqueous solution containing 1 M ammonium metavanadate NH_4VO_3 (99.99% purity, Aldrich) and 2 M oxalic acid ($H_2C_2O_4$, 99.99% purity, Aldrich) in order to control the microstructure of the nanoparticles. The solutions were stirred for 0.5 h at room temperature. The mixture was transferred into a 200 ml Teflon-lined autoclave, and then the autoclave was sealed and maintained at 200ºC for 12 h. The resulting precipitates were washed twice and then dried at 80ºC for 2 h. The crystal structures of the Mo-doped VO_2 particles were characterized by X-ray diffraction (XRD, D8 Advance, Bruker, Germany). The microstructure and chemical composition of Mo-doped VO_2 particles were determined by field emission scanning electron microscopy FE-SEM JSM-6700F (JEOL Techniques, Tokyo, Japan). For the MB degradation test, 0.3 mg Mo-doped VO_2 nanoparticles was added to 30 mL methylene blue solution at pH 10 for varying times. The degradation of MB was determined by UV-Vis (Cary 500 spectroscopy).

Results and discussion. Figures 1 shows an XRD diagram of the Mo-doped VO_2 synthesized by the hydrothermal method with different Mo concentrations. The VO_2 specimen showed several strong peaks, which can be indexed to the VO_2 (B) phase (JCPDS, code 65-7960), as well as a peak corresponding to the (012) plane of the V_2O_3 phase (JCPDS, code 71-280) [15, 16]. However, the Mo-doped VO_2 specimens showed the typical pattern of VO_2 without the V_2O_3 phase (Fig. 1b–d). This result suggests that Mo dopant plays an important role in stabilizing the VO_2 phase in the hydrothermal synthesis process.

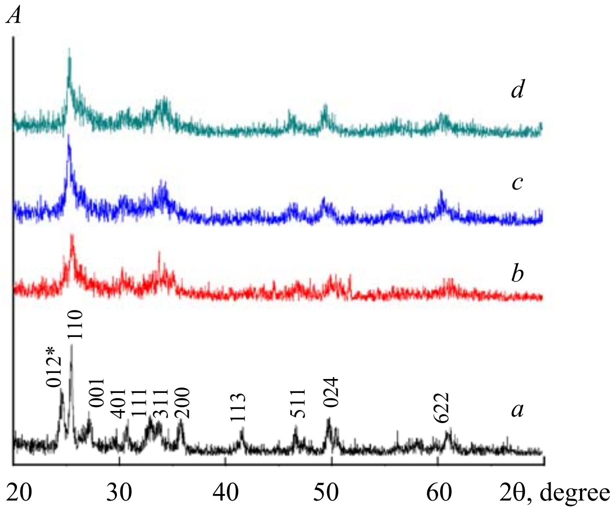

Fig. 1. XRD patterns of Mo-doped VO_2 particles synthesized by the hydrothermal method at 200ºC and time of 12 h. C_{Mo} = 0 (a), 5 (b), 8 (c), and 10 mol.% (d).

The microstructure variation in Mo-doped VO_2 synthesized with different Mo concentrations was examined by SEM, as shown in Fig. 2. Without Mo doping, a dense and smooth nano-plate structure of VO_2 was formed (Fig. 2a), which is similar to that achieved by the hydrothermal processes for VO_2 synthesis [10, 17]. The Mo-doped VO_2 with a Mo concentration of 5 mol.% showed an initial nano-urchin structure formation (Fig. 2b). However, interestingly, the formation of the nano-urchin structure became clearly evident with increase in the Mo concentration to 8 mol.% (Fig. 2c). The formation of nano-urchin structure became more vigorous with increasing Mo concentration to 10 mol.% (Fig. 2d). With a higher Mo doping concentration of 14 and 20 mol.%, the formation of the nano-urchin structure became less evidence (Fig. 2e,f). This suggests the potential use of Mo doping for creation of a unique nano-urchin VO_2 structure by the hydrothermal method. On the basis of these findings, the Mo doping concentration of 10 mol.% was used for further characterizations of the nano-urchin structure.

The morphology of the high nano-urchin structure using a 10 mol.% Mo was more closely examined by FE-SEM. Figure 3a shows a low-magnification FE-SEM image, which clearly shows that most of the particles are VO_2 microspheres with diameters of ~5 μm. The obtained VO_2 microspheres show interesting nano-urchin structures, and the nanowires of the spheres can be clearly seen from the FE-SEM image (Fig. 3b,c). A number of nanowires with very high density were uniformly formed within the grains (Fig. 3d,e). The nano-urchin structure is shown more clearly in high-magnification FE-SEM images in Fig. 3f, which indicates the uniform nanowire distribution with wire diameters of about 500 nm.

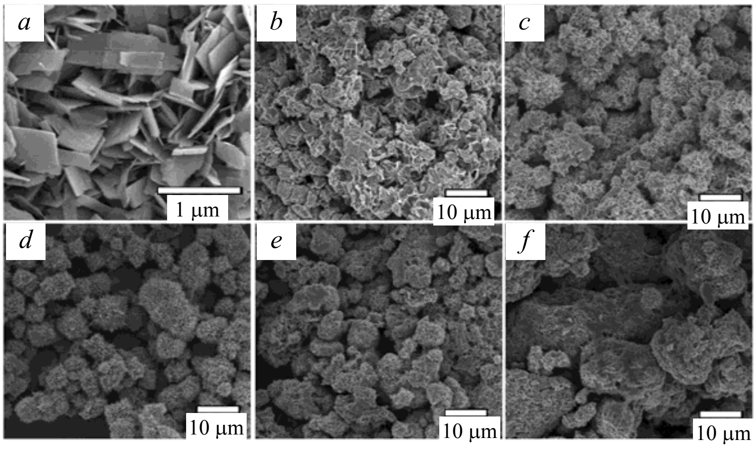

Fig. 2. FE-SEM image showing microstructure of Mo-doped VO_2 synthesized by the hydrothermal method at 200ºC and time of 12 h; C_{Mo} = 0 (a), 5 (b), 8 (c), 10 (d), 14 (e), and 20 mol.% (f).

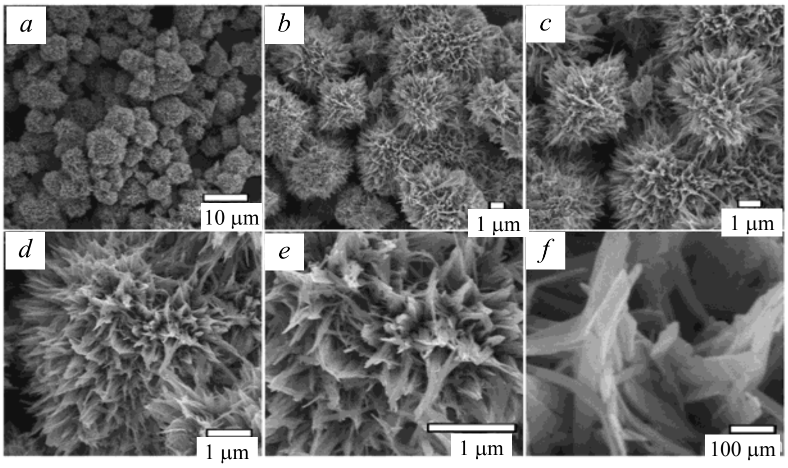

Fig. 3. FE-SEM image showing the nano-urchin structure evolution of Mo-doped VO_2 synthesized by the hydrothermal method (200ºC and time 12 h) with 10 mol.% Mo at different magnifications (a): 1000×, (b): 3000×, (c): 5000×, (d): 10000×, (e): 20000×, and (f): 100000×.

Figure 4 shows the UV-Vis absorption spectra of the original MB and the MB solution after degradation for different times. Original MB has a strong characteristic peak at ~660 nm and one weak absorption peak at ~630 nm. Contacting with nano-urchin Mo-doped VO_2 particles, these absorption peaks become weak and disappear in a very short time of 5 min, demonstrating the effective decolorization of MB. The decolorization percentage increases with time, reaches ~96% after 5 min, and increases to ~98% after 10 min. This MB color degradation characteristic of Mo-doped VO_2 nanoparticles can be attributed mainly to adsorption of MB onto nano-urchin Mo-doped VO_2 particle, resulting in the easy degradation of the MB.

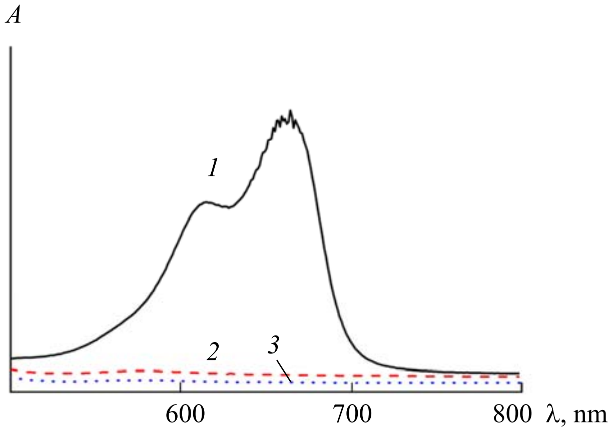

Fig. 4. Decolorization of methylene blue by Mo-doped VO_2 particles;
0 (1), 5 (2), and 10 min (3).

Conclusion. We demonstrated that the nano-urchin Mo-doped VO_2 particles could be obtained effectively by the hydrothermal method. In particular, the nano-urchin Mo doped VO_2 particles were controlled by the Mo concentration. Moreover, nano-urchin Mo-doped VO_2 particles could allow for the fast degradation of methylene blue in a relatively short time of 5–10 min. These findings suggest that the present method is very useful to control the microstructure as well as the dye degradation properties of Mo-doped VO_2 nanoparticles, which would be particular important to environmental engineering in water treatment.

Acknowledgment. This research is funded by the Ministry of Education and Training (MOET) under grant No. B2017-BKA-51.

REFERENCES

1. Y. Zhang, J. Zhang, X. Zhang, Y. Deng, Y. Zhong, C. Huang, X. Liu, X. Liu, S. Mo, *Ceram. Int.*, **39**, 8363–8376 (2013).
2. C. Wu, H. Wei, B. Ning, Y. Xie, *Adv. Mater.*, **22**, 1972–1976 (2010).
3. J. Tian, F. Liu, C. Shen, H. Zhang, T. Yang, L. Bao, X. Wang, D. Liu, H. Li, X. Huang, J. Li, L. Chen, H. Gao, *J. Mater. Res.*, **22**, 1921–1926 (2007).
4. L. Song, Y. Zhang, W. Huang, Q. Shi, D. Li, Y. Zhang, Y. Xu, *Mater. Res. Bull.*, **48**, 2268–2271 (2013).
5. J. Wu, W. Huang, Q. Shi, J. Cai, D. Zhao, Y. Zhang, J. Yan, *Appl. Surf. Sci.*, **268**, 556–560 (2013).
6. T. Okuda, N. Sakamoto, N. Wakiya, H. Miyazaki, T. Ota, H. Suzuki, *J. Jpn Soc. Powder Powder Metall.*, **61**, 99–103 (2014).
7. Z. Cao, X. Xiao, X. Lu, Y. Zhan, H. Cheng, G. Xu, *Sci. Rep.*, **6**, 39154 (2016).
8. P. Phoempoon, L. Sikong, *Sci. World J.*, 2014, 1–8 (2013).
9. S. Ji, Y. Zhao, F. Zhang, P. Jin, S. Ji, Y. Zhao, F. Zhang, P. Jin, *J. Cryst. Growth*, **312**, 282–286 (2010).
10. D. Alie, L. Gedvilas, Z. Wang, R. Tenent, C. Engtrakul, Y. Yan, S. E. Shaheen, A. C. Dillon, C. Ban, *J. Solid State Chem.*, **212**, 237–421 (2014).
11. R. S. Popuri, M. Miclau, A. Artemenko, C. Labrugere, A. Villesuzanne, M. Pollet, *Inorg. Chem.*, **52**, 4780–4785 (2013).
12. M. Li, X. Wu, L. Li, Y. Wang, D. Li, J. Pan, S. Li, L. Sun, G. Li, *J. Mater. Chem. A*, **2**, 4520–4533 (2014).
13. M. K. Chine, F. Sediri, N. Gharbi, *Mater. Res. Bull.*, **47**, 3422–3426 (2012).
14. H. Liu, Y. Gao, J. Zhou, X. Liu, Z. Chen, C. Cao, H. Luo, M. Kanehira, H. Liu, Y. Gao, J. Zhou, X. Liu, Z. Chen, C. Cao, H. Luo, M. Kanehira, *J. Solid State Chem.*, **214**, 79–85 (2014).
15. W. Jiang, J. Ni, K. Yu, Z. Zhu, *Appl. Surf. Sci.*, **257**, 3253–3258 (2011).
16. A. C. Santulli, W. Xu, J. B. Parise, L. Wu, M. C Aronson, F. Zhang, C. Y. Nam, C. T. Black, A. L. Tiano, S. S. Wong, *Phys. Chem. Chem. Phys.*, **21**, 3718–3726 (2009).
17. J. Li, C. Y. Liu, L. J. Mao, *J. Solid State Chem.*, **182**, 2835–2839 (2009).